

## Ester versus Polyketone Formation in the Palladium–Diphosphine Catalyzed Carbonylation of Ethene

Erik Zuidema,<sup>†</sup> Carles Bo,<sup>\*,‡,§</sup> and Piet W. N. M. van Leeuwen<sup>†,‡</sup>

Contribution from the Van't Hoff Institute for Molecular Sciences, Universiteit van Amsterdam, Nieuwe Achtergracht 166, 1018 WV Amsterdam, The Netherlands, Institut Català d'Investigació Química, Avinguda Països Catalans 16, Campus Universitari, 43007 Tarragona, Spain, and Departament de Química Física i Inorgànica, Universitat Rovira i Virgili, Campus Sescelades, Macelli Domingo s/n, 43007 Tarragona, Spain

Received November 24, 2006; E-mail: cbo@iciq.es

**Abstract:** The origin of the chemoselectivity of palladium catalysts containing bidentate phosphine ligands toward either methoxycarbonylation of ethene or the copolymerization of ethene and carbon monoxide was investigated using density functional theory based calculations. For a palladium catalyst containing the electron-donating bis(dimethylphosphino)ethane (dmpe) ligand, the rate determining step for chain propagation is shown to be the insertion of ethene into the metal–acyl bond. The high barrier for chain propagation is attributed to the low stability of the ethene intermediate, (dmpe)Pd(ethene)(C(O)CH<sub>3</sub>). For the competing methanolysis process, the most likely pathway involves the formation of (dmpe)Pd(CH<sub>3</sub>-OH)(C(O)CH<sub>3</sub>) via dissociative ligand exchange, followed by a solvent mediated proton-transfer/reductive-elimination process. The overall barrier for this process is higher than the barrier for ethene insertion into the palladium–acetyl bond, in line with the experimentally observed preference of this type of catalyst toward the formation of polyketone. Electronic bite angle effects on the rates of ethene insertion and ethanoyl methanolysis were evaluated using four electronically and sterically related ligands (Me)<sub>2</sub>P(CH<sub>2</sub>)<sub>n</sub>P(Me)<sub>2</sub> (n = 1–4). Steric effects were studied for larger *tert*-butyl substituted ligands using a QM/MM methodology. The results show that ethene coordination to the metal center and subsequent insertion into the palladium–ethanoyl bond are disfavored by the addition of steric bulk around the metal center. Key intermediates in the methanolysis mechanism, on the other hand, are stabilized because of electronic effects caused by increasing the bite angle of the diphosphine ligand. The combined effects explain successfully which ligands give polymer and which ones give methyl propionate as the major products of the reaction.

### 1. Introduction

Palladium catalyzed carbon–carbon and carbon–heteroatom bond forming processes have become an essential tool in the industrial production of a wide variety of organic compounds.<sup>1</sup> To elucidate the mechanisms involved in these important processes, they have been the subject of many mechanistic and theoretical studies. While early studies focused on carbon–carbon and carbon–hydrogen bond formation,<sup>2</sup> the experimental scope of these processes has now been extended to include reactions involving carbon–oxygen,<sup>3</sup> carbon–nitrogen,<sup>4</sup> and carbon–sulfur<sup>5</sup> bond formation.

Only recently have theoretical studies started to address the mechanisms behind these heteroatomic coupling reactions.<sup>6,7</sup> In one study, we showed that the rate of reductive C–X (X = C, O) bond formation involving palladium–diphosphine complexes is highly dependent on the nature of the two reacting moieties.<sup>7</sup> In the reductive elimination of methyl ethanoate from (diphosphine)Pd(OMe)(C(O)CH<sub>3</sub>), a reaction believed to be the product forming step in the methoxycarbonylation/alkene–CO copoly-

<sup>†</sup> Universiteit van Amsterdam.

<sup>‡</sup> Institut Català d'Investigació Química.

<sup>§</sup> Universitat Rovira i Virgili.

- (1) (a) Negishi, E. I. *Handbook of Organopalladium Chemistry for Organic Synthesis*; John Wiley & Sons Inc.: New York, 2002. (b) Schlummer, B.; Scholz, U. *Adv. Synth. Catal.* **2004**, *346*, 1599. (c) Tsuji, J. *Palladium in Organic Synthesis*; Springer-Verlag: Berlin, 2005.
- (2) (a) Gillie, A.; Stille, J. K. *J. Am. Chem. Soc.* **1980**, *102*, 4933. (b) Moravskiy, A.; Stille, J. K. *J. Am. Chem. Soc.* **1981**, *103*, 4182. (c) Tatsumi, K.; Hoffmann, R.; Yamamoto, A.; Stille, J. K. *Bull. Chem. Soc. Jpn.* **1981**, *54*, 1857. (d) Balazs, A. C.; Johnson, K. H.; Whitesides, G. M. *Inorg. Chem.* **1982**, *21*, 2162. (e) Low, J. J.; Goddard, W. A. *Organometallics* **1986**, *4*, 609. (f) Low, J. J.; Goddard, W. A., III. *J. Am. Chem. Soc.* **1986**, *108*, 6115. (g) Calhorda, M. J.; Brown, J. M.; Cooley, N. A. *Organometallics* **1991**, *10*, 1431. (h) Dedieu, A. *Chem. Rev.* **2000**, *100*, 543.

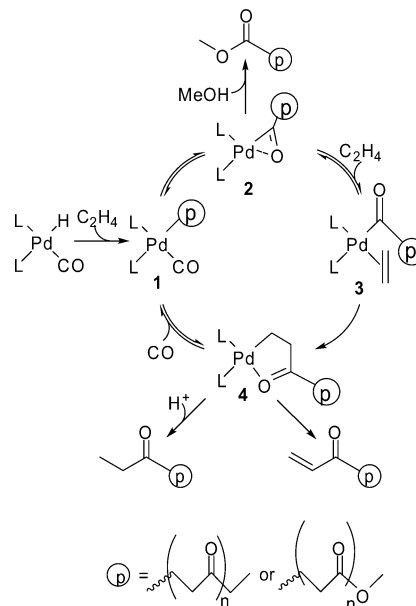
- (3) (a) Mann, G.; Incarvito, C.; Rheingold, A. L.; Hartwig, J. F. *J. Am. Chem. Soc.* **1999**, *121*, 3224. (b) Mann, G.; Shelby, Q.; Roy, A. H.; Hartwig, J. F. *Organometallics* **2003**, *22*, 2775. (c) Vorogushin, A. V.; Huang, X. H.; Buchwald, S. L. *J. Am. Chem. Soc.* **2005**, *127*, 8146.
- (4) (a) Driver, M. S.; Hartwig, J. F. *J. Am. Chem. Soc.* **1997**, *119*, 8232. (b) Leitner, A.; Shu, C. T.; Hartwig, J. F. *Org. Lett.* **2005**, *7*, 1093. (c) Shen, Q. L.; Shekhar, S.; Stambuli, J. P.; Hartwig, J. F. *Angew. Chem., Int. Ed.* **2005**, *44*, 1371. (d) Anderson, K. W.; Tundel, R. E.; Ikawa, T.; Altman, R. A.; Buchwald, S. L. *Angew. Chem., Int. Ed.* **2006**, *45*, 6523. (e) Shekhar, S.; Ryberg, P.; Hartwig, J. F.; Mathew, J. S.; Blackmond, D. G.; Strieter, E. R.; Buchwald, S. L. *J. Am. Chem. Soc.* **2006**, *128*, 3584.
- (5) (a) Mann, G.; Baranano, D.; Hartwig, J. F.; Rheingold, A. L.; Guzei, I. A. *J. Am. Chem. Soc.* **1998**, *120*, 9205. (b) Fernandez-Rodriguez, M. A.; Shen, Q. L.; Hartwig, J. F. *Chem.–Eur. J.* **2006**, *12*, 7782. (c) Fernandez-Rodriguez, M. A.; Shen, Q. L.; Hartwig, J. F. *J. Am. Chem. Soc.* **2006**, *128*, 2180.
- (6) Macgregor, S. A.; Neave, G. W.; Smith, C. *Faraday Discuss.* **2003**, *124*, 111.
- (7) Zuidema, E.; Van Leeuwen, P. W. N. M.; Bo, C. *Organometallics* **2005**, *24*, 3703.

erization reaction,<sup>8–11</sup> we observed an extremely facile carbon–oxygen bond forming process. This was attributed to a highly effective donor–acceptor type migratory reductive elimination process involving the oxygen lone pair of the methoxy moiety and the  $\pi^*$ -orbital of the acetyl moiety.

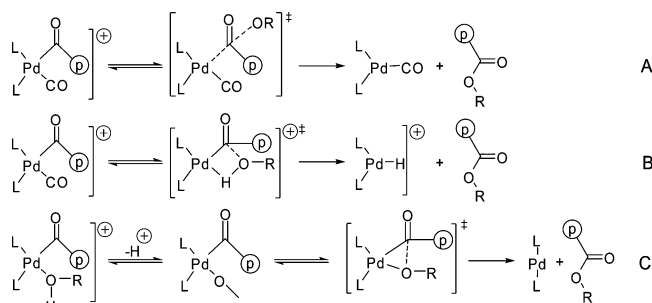
These observations seem to be in good agreement with the development of several highly active and selective catalyst systems for the formation of methyl propionate via the methoxycarbonylation of ethene.<sup>12,13</sup> However, several structurally related catalyst systems have been reported that suppress ester formation and consequently exclusively produce high-molecular-weight copolymers under identical reaction conditions.<sup>8,14</sup> Although it is clear from these studies that the choice of bidentate ligand is crucial in determining the product distribution of the reaction, the factors governing the chemoselectivity of a catalyst system in this reaction are as yet unclear.

Because of the industrial importance of the copolymerization reaction, the mechanism for the palladium–diphosphine catalyzed formation of alkene–carbon monoxide copolymers has been the subject of intensive experimental<sup>15–21</sup> and theoretical<sup>22–24</sup> study, and the process is now well understood (Scheme 1). Until recently, the competing chain termination processes received relatively little attention,<sup>10,25,26</sup> despite their clear importance in determining the product distribution of the reaction. A number

**Scheme 1.** Mechanism of the Palladium-Catalyzed Reaction between Alkenes and Carbon Monoxide, Including Initiation and Termination Pathways



**Scheme 2.** Proposed Mechanisms for the Solvolysis of Palladium–Acyl Complexes



of termination processes have been identified, including protonolysis or  $\beta$ -hydride elimination of alkyl complex **4** and solvolysis of acyl complex **2** (Scheme 1). These termination processes may operate in parallel, although for very active hydroxy- and methoxycarbonylation catalysts it has been shown that chain termination occurs exclusively through the solvolysis of palladium–acyl complex **2**.<sup>18</sup>

The mechanism of carbon–oxygen bond formation through solvolysis of acyl complex **2** remains heavily debated. Initially it was believed that, similar to the solvolysis of acid chlorides, solvolysis of palladium–acyl complexes proceeds via a direct intermolecular attack of the (deprotonated) alcoholic solvent on the carbonyl moiety of the acyl group<sup>8</sup> (reaction A in Scheme 2). This mechanism was invoked to explain the high selectivity of palladium catalysts modified by two monodentate ligands toward the alkoxy carbonylation of alkenes. It was argued that the trans coordination of the two monodentate ligands prevented fast insertion of alkene and carbon monoxide into the polymer

- (8) Drent, E.; Budzelaar, P. H. M. *Chem. Rev.* **1996**, *96*, 663.  
 (9) Sen, A. *Catalytic Synthesis of Alkene-Carbon Monoxide Copolymers and Cooligomers*; Kluwer Academic Publishers: Dordrecht, The Netherlands, 2003.  
 (10) Van Leeuwen, P. W. N. M.; Zuideveld, M. A.; Swennenhuis, B. H. G.; Freixa, Z.; Kamer, P. C. J.; Goubitz, K.; Fraanje, J.; Lutz, M.; Spek, A. L. *J. Am. Chem. Soc.* **2003**, *125*, 5523.  
 (11) Freixa, Z.; Van Leeuwen, P. W. N. M. *J. Chem. Soc., Dalton Trans.* **2003**, *10*, 1890.  
 (12) (a) Drent, E.; Kragt, E. Shell International Research. EP495,548, 1992. (b) Eastham, G. R.; Tooze, R. P.; Wang, X. L.; Whiston, K. WO 96/19434, ICI, 1996. (c) Drent, E.; Pringle, P. G.; Suykerbuyk, J. C. L. J. Shell International Research. WO 98/42717, 1998. (d) Gee, V.; Orpen, A. G.; Phatmung, H.; Pringle, P. G.; Pugh, R. I. *J. Chem. Soc., Chem. Commun.* **1999**, 901.  
 (13) Clegg, W.; Eastham, G. R.; Elsegood, M. R. J.; Tooze, R. P.; Wang, X. L.; Whiston, K. *J. Chem. Soc., Chem. Commun.* **1999**, 1877.  
 (14) (a) Bianchini, C.; Meli, A. *Coord. Chem. Rev.* **2002**, *225*, 35. (b) Mul, W. P.; Van der Made, A. W.; Smaardijk, A. A.; Drent, E. In *Catalytic Synthesis of Alkene-Carbon Monoxide Copolymers and Cooligomers*; Sen, A., Ed.; Kluwer Academic Publishers: Dordrecht, The Netherlands, 2003.  
 (15) (a) Drent, E.; Van Broekhoven, J. A. M.; Doyle, M. J. *J. Organomet. Chem.* **1991**, *417*, 235. (b) Eastham, G. R.; Heaton, B. T.; Iggo, J. A.; Tooze, R. P.; Whyman, R.; Zacchini, S. *J. Chem. Soc., Chem. Commun.* **2000**, 609. (c) Eastham, G. R.; Tooze, R. P.; Kilner, M.; Foster, D. F.; Cole-Hamilton, D. J. *J. Chem. Soc., Dalton Trans.* **2002**, 1613. (d) Wolowska, J.; Eastham, G. R.; Heaton, B. T.; Iggo, J. A.; Jacob, C.; Whyman, R. *J. Chem. Soc., Chem. Commun.* **2002**, 2784. (e) Brumbaugh, J. S.; Wittle, R. R.; Parvez, M.; Sen, A. *Organometallics* **1990**, *9*, 1735. (f) Rix, F. C.; Brookhart, M. *J. Am. Chem. Soc.* **1995**, *117*, 1137. (g) Rix, F. C.; Brookhart, M.; White, P. S. *J. Am. Chem. Soc.* **1996**, *118*, 4746. (h) Shultz, C. S.; Ledford, J.; DeSimone, J. M.; Brookhart, M. *J. Am. Chem. Soc.* **2000**, *122*, 6351. (i) Dekker, G. P. C. M.; Elsevier, C. J.; Vrieze, K.; Van Leeuwen, P. W. N. M. *Organometallics* **1992**, *11*, 1598. (j) Toth, I.; Elsevier, C. J. *J. Am. Chem. Soc.* **1993**, *115*, 10388. (k) Kayaki, Y.; Kawataka, F.; Shimizu, I.; Yamamoto, A. *Chem. Lett.* **1994**, 2171. (l) Markies, B. A.; Wijkens, P.; Dedieu, A.; Boersma, J.; Spek, A. L.; Van Koten, G. *Organometallics* **1995**, *14*, 5628. (m) Kayaki, Y.; Shimizu, I.; Yamamoto, A. *Bull. Chem. Soc. Jpn.* **1997**, *70*, 917. (n) Ledford, J.; Shultz, C. S.; Gates, D. P.; White, P. S.; DeSimone, J. M.; Brookhart, M. *Organometallics* **2001**, *20*, 5266.  
 (16) Clegg, W.; Eastham, G. R.; Elsegood, M. R. J.; Heaton, B. T.; Iggo, J. A.; Tooze, R. P.; Whyman, R.; Zacchini, S. *Organometallics* **2002**, *21*, 1832.  
 (17) Liu, J.; Heaton, B. T.; Iggo, J. A.; Whyman, R. *Angew. Chem., Int. Ed.* **2004**, *43*, 90.  
 (18) Liu, J.; Heaton, B. T.; Iggo, J. A.; Whyman, R.; Bickley, J. F.; Steiner, A. *Chem.—Eur. J.* **2006**, *12*, 4417.  
 (19) Dekker, G. P. C. M.; Elsevier, C. J.; Vrieze, K.; Van Leeuwen, P. W. N. M.; Roobeek, C. F. J. *Organomet. Chem.* **1992**, *430*, 357.  
 (20) Shultz, C. S.; Ledford, J.; DeSimone, J. M.; Brookhart, M. *Organometallics* **2001**, *20*, 5266.  
 (21) Shen, H.; Jordan, R. F. *Organometallics* **2003**, *22*, 1878.  
 (22) Margl, P.; Ziegler, T. *J. Am. Chem. Soc.* **1996**, *118*, 7337.  
 (23) Svensson, M.; Matsubara, T.; Morokuma, K. *Organometallics* **1996**, *15*, 5568.  
 (24) Margl, P.; Ziegler, T. *Organometallics* **1996**, *15*, 5519.

- (25) (a) Toth, I.; Elsevier, C. J. *Organometallics* **1994**, *13*, 2118. (b) Ozawa, F.; Kawasaki, N.; Okamoto, H.; Yamamoto, T.; Yamamoto, A. *Organometallics* **1987**, *6*, 1640. (c) Zuideveld, M. A.; Kamer, P. C. J.; Van Leeuwen, P. W. N. M.; Klusener, P. A. A.; Stil, H. A.; Roobeek, C. F. J. *Am. Chem. Soc.* **1998**, *120*, 7977.  
 (26) Bianchini, C.; Meli, A.; Oberhauser, W.; Van Leeuwen, P. W. N. M.; Zuideveld, M. A.; Freixa, Z.; Kamer, P. C. J.; Spek, A. L.; Gusev, O. V.; Kal'sin, A. M. *Organometallics* **2003**, *22*, 2409.

chain, eventually leading to intermolecular alcoholysis. Cole-Hamilton and co-workers have suggested that the unusual high rate of alcoholysis observed for bulky bidentate phosphine ligands can be explained by decoordination of one of the diphosphine arms, thereby enhancing the susceptibility of the acyl-moiety toward intermolecular solvolysis.<sup>27</sup>

In the past decade, however, evidence has been collected that suggests that the metal center is directly involved in the solvolysis process. Our group has demonstrated that the rate of methanolysis of palladium–ethanoyl complexes containing bidentate diphosphine ligands is highly dependent on the bite angle of the ligand. While *cis*-coordinating diphosphine ligands led to extremely fast methanolysis, rigid *trans*-coordinating ligands completely inhibited methanolysis of the palladium–ethanoyl species **2**.<sup>10</sup> Van Leeuwen and co-workers have collected similar evidence that methanolysis of [Pd(dppomf)-(C(O)CH<sub>3</sub>)]OTf requires prior rearrangement of the diphosphine ligand from a *trans*- $\kappa$ -P,P,Fe-coordination to a *cis*- $\kappa$ -P,P-coordination.<sup>26</sup> More recently, Whyman and co-workers have reported that methanolysis of palladium–ethanoyl complexes containing electron-donating bidentate ligands also required a vacant coordination site adjacent to the acyl moiety.<sup>17</sup>

On the basis of these experimental observations, mechanisms have been proposed in which an incoming solvent molecule interacts with the palladium center during the solvolysis process (mechanisms B and C in Scheme 2). In mechanism B, palladium–acyl complex **2** reacts with a solvent molecule via a metathesis-type reaction in which the carbon–oxygen and palladium–hydride bond are formed simultaneously. In mechanism C, the solvent molecule coordinates to the palladium center, followed by deprotonation of the coordinated solvent species. In the final step of this mechanism, a reductive elimination reaction liberates the final product. Similar reaction mechanisms have been proposed for other carbon–heteroatom bond-forming reactions, such as the C–X bond forming reactions developed by Buchwald and Hartwig.<sup>28</sup> Clearly, both mechanisms B and C explain why solvolysis requires *cis* coordination of the spectator diphosphine ligand. Furthermore, mechanism B also explains the high rate of methanolysis observed for electron-rich palladium–acyl complexes; the high electron density at the metal center facilitates the deprotonation of the solvent molecule during the solvolysis reaction.

Since both carbon–carbon and carbon–oxygen bond-forming steps in this palladium catalyzed reaction require *cis* coordination of the substrate and the growing copolymer chain, it is not surprising that the application of *cis*-coordinating bidentate phosphine ligands has proven to be successful in the production of both low-molecular-weight esters and high-molecular-weight copolymer. The large differences in chemoselectivity between catalysts containing structurally similar *cis* coordinating diphosphine ligands, however, remain largely unexplained.<sup>11</sup>

In our previous experimental contribution on the methanolysis process we noted that, depending on the ligands used in the reaction, the rate of the carbon–oxygen bond formation may vary by at least 8 orders of magnitude.<sup>10</sup> The C–O ester bond

formation was described as a migratory reductive elimination, typical of such heterobond formations in palladium-catalyzed reactions,<sup>29</sup> such as the Buchwald–Hartwig amination reactions.<sup>30,31</sup> The steric bulk of bidentate phosphines was singled out as the cause for fast C–O bond formation, while the effect of a wide bite angle remained unproven.<sup>11</sup> For C–X bond formation from PdX(hydrocarbyl) complexes, however, there is convincing experimental and theoretical evidence<sup>7,31,32</sup> that wider bite angles promote reductive eliminations, which may also exceed orders of magnitude.

Here we present a theoretical study into the origin of the chemoselectivity of palladium catalyst systems toward either carbon monoxide/ethene copolymerization or the methoxycarbonylation of ethene. This study focuses on the steps involved in chain propagation via the alternating insertion of ethene and carbon monoxide into the palladium–carbon bond, as well as mechanisms involved in carbon–oxygen bond-forming methanolysis of  $\eta^2$ -palladium–acyl complex **2**. In the second part, the effect of the natural bite angle and the steric bulk of the diphosphine ligand on the rate of carbon–carbon and carbon–oxygen bond formation is addressed by comparing the relative rates of chain propagation and chain termination for electronically identical diphosphine ligands (R)<sub>2</sub>P(CH<sub>2</sub>)<sub>n</sub>P(R)<sub>2</sub> (*n* = 1–4, R = Me, *t*-Bu).

## 2. Results and Discussion

**2.1. Chain Propagation Mechanism.** The reaction steps and intermediates involved in chain propagation via the alternating insertion of carbon monoxide and ethene into the growing polymer chain have previously been investigated using computational techniques for catalyst systems containing bidentate imine<sup>23</sup> and electron-poor diphosphine ligands.<sup>22,24</sup> We have investigated the insertion of carbon monoxide into the palladium–alkyl bond, the formation of ethene complexes, and the subsequent insertion of ethene into the palladium–acyl bond for a catalyst system containing the electron-donating bidentate (Me)<sub>2</sub>P(CH<sub>2</sub>)<sub>2</sub>P(Me)<sub>2</sub> ligand. The reaction pathways considered in this study are shown in Scheme 3. The calculated relative gas-phase energies, relative energies in methanol, and Gibbs free energies relative to complex **6** are summarized in Table 1

Analogous to previous mechanistic studies from our group and others, cationic palladium–methyl complex **1** was chosen as a starting point for our investigations. Methyl complex **1** can undergo direct migratory insertion of carbon monoxide into the palladium–alkyl bond via transition-state **TS1**, generating three-coordinate ethanoyl species **2**. Subsequent coordination of carbon monoxide to species **2** yields carbonyl complex **6**, which for most methoxycarbonylation catalyst systems is the resting state of the catalyst. The calculated structures for complexes **1**, **2**, and **6** and transition-state **TS1** are very similar to structures previously reported by Ziegler and co-workers for palladium

- (27) Cole-Hamilton, D. J.; Robertson, R. A. M. In *Catalytic Synthesis of Alkene-Carbon Monoxide Copolymers and Cooligomers*; Sen, A., Ed.; Kluwer Academic Publishers: Dordrecht, The Netherlands, 2003.  
(28) (a) Paul, F.; Patt, J.; Hartwig, J. F. *J. Am. Chem. Soc.* **1994**, *116*, 5969. (b) Driver, M. S.; Hartwig, J. F. *J. Am. Chem. Soc.* **1995**, *117*, 4708. (c) Hartwig, J. F. *Acc. Chem. Res.* **1998**, *31*, 852.

- (29) Baranano, D.; Hartwig, J. F. *J. Am. Chem. Soc.* **1995**, *117*, 2937.  
(30) (a) Widenhoefer, R. A.; Zhong, H. A.; Buchwald, S. L. *J. Am. Chem. Soc.* **1997**, *119*, 6787. (b) Widenhoefer, R. A.; Buchwald, S. L. *J. Am. Chem. Soc.* **1998**, *120*, 6504.  
(31) Hamann, B. C.; Hartwig, J. F. *J. Am. Chem. Soc.* **1998**, *120*, 3694.  
(32) (a) Brown, J. M.; Guiry, P. J. *Inorg. Chim. Acta* **1994**, *220*, 249. (b) Marcone, J. E.; Moloy, K. G. *J. Am. Chem. Soc.* **1998**, *120*, 8527. (c) Albaneze-Walker, J.; Bazaral, C.; Leavey, T.; Dormer, P. G.; Murry, J. A. *Org. Lett.* **2004**, *6*, 2097. (d) Fujita, K.; Yamashita, M.; Puschmann, F.; Alvarez-Falcon, M. M.; Incarvito, C. D.; Hartwig, J. F. *J. Am. Chem. Soc.* **2006**, *128*, 9044. (e) Martinelli, J. R.; Freckmann, D. M. M.; Buchwald, S. L. *Org. Lett.* **2006**, *8*, 4843.

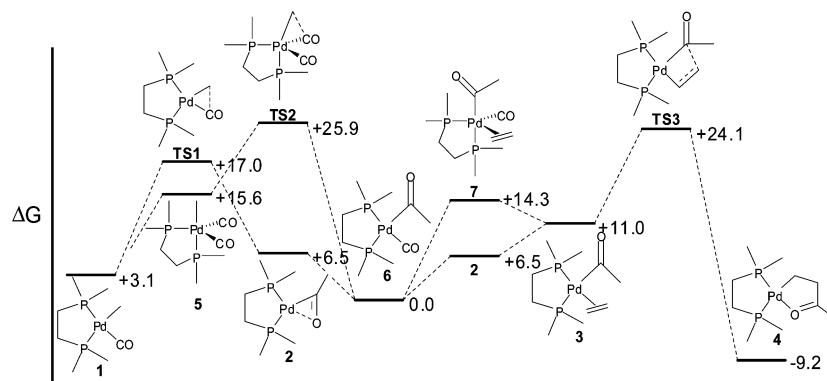


**Figure 1.** Gas-phase Gibbs free energy profile of the initial steps of the copolymerization of carbon monoxide and ethene, for a catalyst containing the  $(\text{Me})_2\text{P}(\text{CH}_2)_2\text{P}(\text{Me})_2$  ligand system, determined at 1 atm of pressure and 298.15 K.

**Scheme 3.** Reaction Pathways Involved in the Chain-Propagation Mechanism

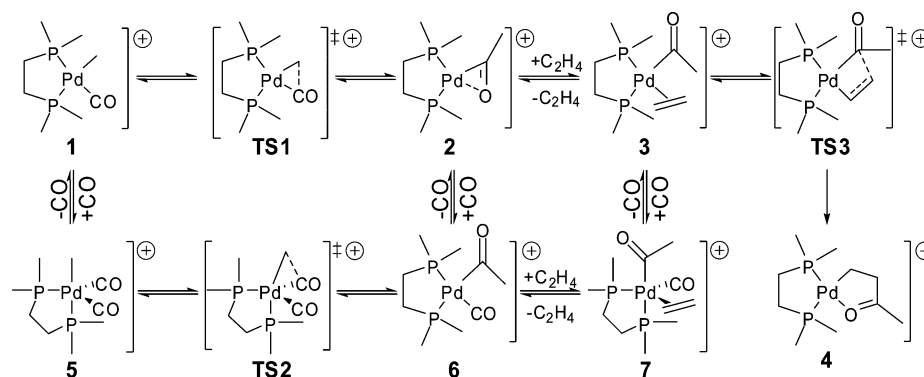


**Table 1.** Relative Energies and Gibbs Free Energies of Structures Containing  $(\text{Me})_2\text{P}(\text{CH}_2)_2\text{P}(\text{Me})_2$  Involved in the Initial Steps of the Copolymerization of Carbon Monoxide and Ethene<sup>a</sup>

	1	TS1	2	5	TS2	6	7	3	TS3	4
$\Delta E_g$	19.4	33.1	20.0	15.8	28.5	0.0	-0.9	8.0	21.0	-10.9
$\Delta E_{\text{MeOH}}^b$	21.7	35.1	22.1	17.7	30.8	0.0	0.9	9.3	22.8	-5.9
$\Delta G^c$	3.1	17.0	6.5	15.6	25.9	0.0	14.3	11.0	24.1	-9.2

<sup>a</sup> Energy values are reported relative to complex **6** in  $\text{kcal mol}^{-1}$ .  
<sup>b</sup> Relative energies in methanol, calculated from gas-phase optimized structures using the conductor-like screening model. <sup>c</sup> Gas-phase Gibbs free energies were evaluated at 1 atm of pressure and at 298.15 K.

complexes containing the less electron-donating  $\text{H}_2\text{PCH}=\text{CHPH}_2$  ligand.<sup>22</sup> The insertion reaction proceeds with a moderate energy barrier of  $13.7 \text{ kcal mol}^{-1}$  (Figure 1). In contrast to results for the less electron-donating  $\text{H}_2\text{PCH}=\text{CHPH}_2$  ligand system, complex **2** is less stable than complex **1**. The coordination of carbon monoxide to species **2**, forming complex **6**, provides the driving force for the reaction. The coordination proceeds without barrier and is exothermic by  $20.0 \text{ kcal mol}^{-1}$ .

It has previously been shown for related nickel complexes<sup>33</sup> and palladium complexes bearing bidentate and tridentate nitrogen-based ligands<sup>34</sup> that the mechanism for CO insertion may involve coordination of a fifth ligand to the metal center prior to insertion of the CO moiety into the metal–alkyl bond. In our case, carbon monoxide readily coordinates to the electron-rich metal center of complex **1**, yielding stable trigonal bipyramidal complex **5**. CO insertion then proceeds through

transition-state **TS2**, forming carbonyl complex **6** directly. The structure of this transition state is distorted square pyramidal, the CO ligand not involved in the reaction occupying the axial position of the complex. The activation energy associated with this insertion process is  $12.7 \text{ kcal mol}^{-1}$ ,  $1.0 \text{ kcal mol}^{-1}$  lower than the activation energy for direct CO insertion via transition-state **TS1**. The calculated Gibbs free energies for the intermediates in the two CO-insertion pathways suggest, however, that CO coordination prior to insertion is not favorable under the experimental conditions, mainly because of loss of entropy while forming complex **5**. It is predicted that carbon monoxide insertion proceeds via transition-state **TS1**, with a free energy barrier of  $13.9 \text{ kcal mol}^{-1}$ . On the basis of the small difference in the free energies of methyl complex **1** and ethanoyl–carbonyl complex **6** and the modest activation energy of the CO-insertion process, carbon monoxide insertion into the palladium–alkyl bond is predicted to be readily reversible, in line with experimental observations for several palladium–diphosphine catalyst systems.<sup>10</sup>

Carbonyl complex **6** is in equilibrium with ethene complex **3** through dissociative (via complex **2**) or associative carbon monoxide–ethene ligand exchange processes. For associative carbon monoxide–ethene exchange, stable trigonal bipyramidal intermediate **7** was obtained. In this complex, the  $\pi$ -accepting carbon monoxide and ethene ligand occupy the equatorial plane and the ethanoyl moiety is located in one of the axial positions. The bidentate diphosphine ligand adopts an equatorial-axial coordination mode. Other geometries, where the ethanoyl moiety is coordinated in the equatorial plane did not yield stable trigonal bipyramidal structures. Invariably, the third equatorial ligand (CO, ethene) decoordinated during the geometry optimization

(33) Angelis, F. D.; Sgamellotti, A. *Organometallics* **2002**, *21*, 2036.

(34) (a) Blomberg, M. R. A.; Karlson, C. A. M.; Siegbahn, P. E. M. *J. Phys. Chem.* **1993**, *97*, 9341. (b) Nakajima, T.; Hirao, K. *Chem. Phys. Lett.* **1999**, *302*, 383. (c) Nakajima, T.; Suzumara, T.; Hirao, K. *Chem. Phys. Lett.* **1999**, *302*, 271.

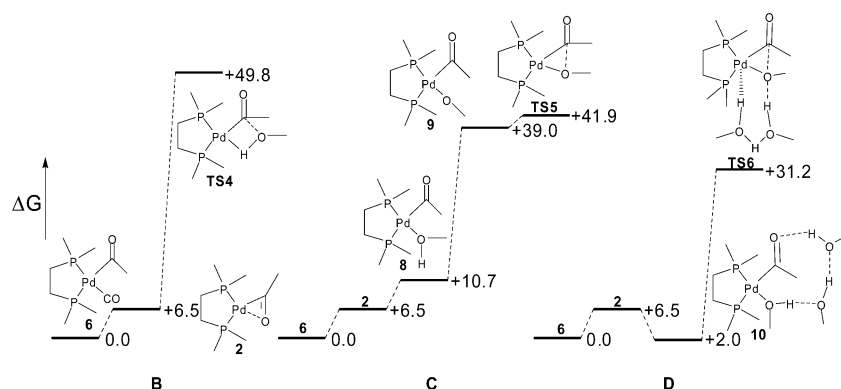


**Figure 2.** Gas-phase Gibbs free-energy profiles of methanolysis mechanisms B (left), C (middle), and D (right) for a catalyst containing the  $(\text{Me})_2\text{P}(\text{CH}_2)_2\text{P}(\text{Me})_2$  ligand system, determined at 1 atm of pressure and 298.15 K.

process, leading to square planar complexes. For the larger *dmph* ligand system (vide infra), bisequatorial coordination of the diphosphine was considered, but the lowest energy structure containing a bisequatorial coordinated diphosphine ligand was 2.1 kcal mol<sup>-1</sup> higher in energy than the structure containing an equatorial-axial coordinated ligand. Therefore, it seems that the presence of at least two  $\pi$ -accepting ligands in the equatorial plane of these electron-rich complexes is a prerequisite for the generation of stable penta-coordinated intermediates.

The low relative energy of complex **7** compared to  $\eta^2$ -acyl intermediate **2** suggests that CO-ethene exchange occurs in an associative fashion. However, when the Gibbs free energies of the complexes are compared,  $\eta^2$ -acyl complex **2** is stabilized relative to penta-coordinated complex **7**, mainly because of the incorporation of entropic effects. For electron-withdrawing ligand systems, which are less effective in stabilizing  $\eta^2$ -acyl complex **2**, we cannot exclude the possibility that ethene complex **3** is formed through an associative ligand exchange pathway.

In contrast to previous results for the less electron-donating  $\text{H}_2\text{PCH}=\text{CHPH}_2$  ligand system, reported by Ziegler and co-workers, the lowest energy structure of ethene complex **3** containing the *dmpe* ligand system exhibits an in-plane coordination mode of the ethene moiety. It has been shown that this in-plane coordination mode is generally preferred for Pd(0)-alkene complexes, maximizing back-donation from the electron-rich metal center to the ethene moiety. In square planar Pd(II) complexes, where back-donation from the metal to the ligand is usually less extensive, the ethene moiety is generally coordinated perpendicular to the plane of the complex.<sup>35</sup> We attribute the unusual in-plane coordination mode of the ethene ligand in Pd(II) complex **3** to the unusual electronic and steric properties of the *dmpe* ligand system. The electron-donating diphosphine ligand induces considerable back-donation from the metal center to the ethene ligand in the plane of the complex, while it does not induce sufficient steric repulsion to enforce out-of-plane coordination of the ethene moiety in complex **3**. Note that ethene complex **3** is considerably less stable than carbonyl complex **6**. A relative energy of 8.0 kcal mol<sup>-1</sup> and a relative free energy of 11.0 kcal mol<sup>-1</sup> are predicted for ethene complex **3**.

Formation of ethene complex **3** is followed by insertion of the coordinated ethene moiety into the palladium–ethanoyl bond, via transition-state **TS3**. The process proceeds with an energy barrier of 13.0 kcal mol<sup>-1</sup> and a free energy barrier of

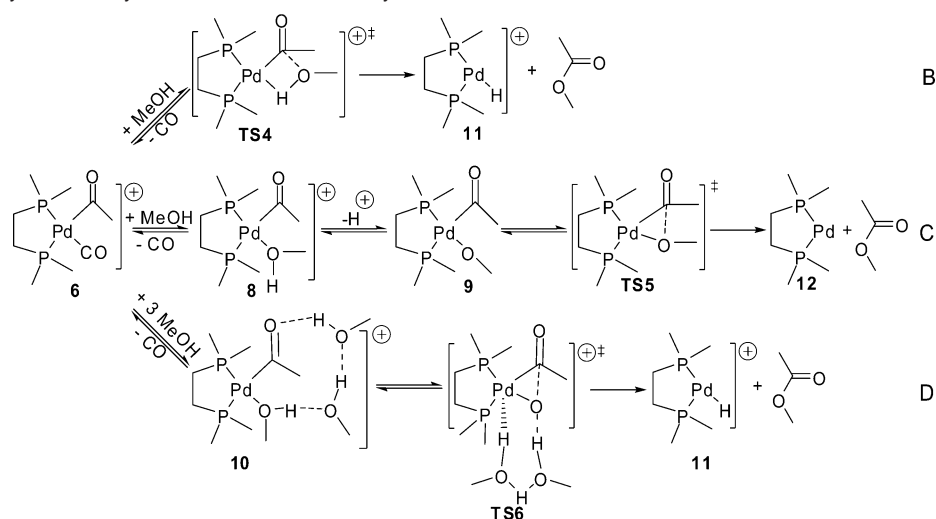
13.1 kcal mol<sup>-1</sup>. Both values compare favorably to experimentally determined activation energy of 12.3 kcal mol<sup>-1</sup> for the insertion of ethene in  $(\text{dppp})\text{Pd}(\text{ethene})(\text{COCH}_3)$ ,<sup>20</sup> reported by Shultz et al. The calculated activation energy for ethene insertion starting from ethene complex **3** is lower than the activation energy predicted for carbon monoxide insertion starting from complex **1**. The low stability of ethene complex **3** relative to carbonyl complex **6**, however, increases the overall free energy barrier for ethene insertion considerably. For this ligand system, the process proceeds with an overall barrier of 21.0 kcal mol<sup>-1</sup> and a free energy barrier of 24.1 kcal mol<sup>-1</sup>. In agreement with experimental observations,<sup>36</sup> ethene insertion is predicted to be the rate determining step in the chain propagation process; the free energy of ethene insertion transition-state **TS3** is 7.1 kcal mol<sup>-1</sup> higher than the free energy of CO insertion transition-state **TS1**.

The low Gibbs free energy of  $\beta$ -chelate complex **4** relative to carbonyl complex **6** suggests that for this copolymerization catalyst, complex **4** is the resting state of the catalyst, in line with experimental observations for other copolymerization catalyst systems. Because of the high stability of complex **4** and the high barrier for ethene insertion via transition-state **TS3**, ethene insertion into the palladium–ethanoyl bond is essentially irreversible under the experimental conditions. Consequently, the chemoselectivity of the catalyst toward either copolymerization or methoxycarbonylation is determined by the respective barriers for ethene insertion and methanolysis of carbonyl complex **6**.

**2.2. Methanolysis Mechanisms.** While the mechanism of chain propagation through ethene insertion into palladium–acyl bonds is well understood, the mechanism of the competing chain termination process, the methanolysis of palladium–acyl complexes, remains heavily debated. On the basis of the available literature (vide supra), three reaction pathways were considered in this study (Scheme 4). In addition to the two pathways B and C shown in Scheme 2, a possible solvent-assisted concerted proton-transfer/reductive-elimination pathway (D) was considered. The relative energies, energies in methanol and (gas-phase) Gibbs free energies of the intermediates involved in these reactions are summarized in Table 2. The free energy profiles of the three methanolysis pathways are shown in Figure 2. For

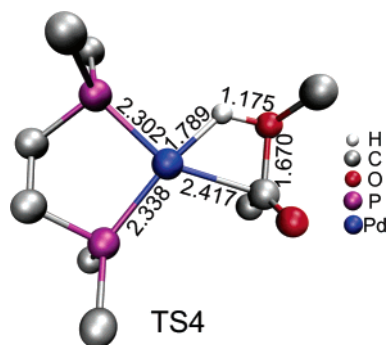
(35) Kurosawa, H.; Ikeda, I. *J. Organomet. Chem.* **1992**, 428, 289.

(36) (a) Fatutto, D.; Toniolo, L.; Chaudhari, R. V. *Cat. Today* **1999**, 48, 49. (b) Mul, W. P.; Oosterbeek, H.; Beitel, G. A.; Kramer, H. J.; Drent, E. *Angew. Chem., Int. Ed.* **2000**, 39, 1848.

**Scheme 4.** Methanolysis Pathways Considered in This Study**Table 2.** Relative Energies and Gibbs Free Energies of Complexes Involved in the Methanolysis of Complex **6** for the (Me)<sub>2</sub>P(CH<sub>2</sub>)<sub>2</sub>P(Me)<sub>2</sub> Ligand System<sup>a</sup>

	<b>2</b>	<b>TS4</b>	<b>8</b>	<b>9</b>	<b>TS5</b>	<b>10</b>	<b>TS6</b>
$\Delta E_g$	20.0	55.8	9.3	41.0	43.3	-0.6	34.2
$\Delta E_{\text{MeOH}}^b$	22.1	63.4	14.6	38.9	40.5	9.0	42.1
$\Delta G^c$	6.5	49.8	10.7	39.0	41.9	2.0	31.2

<sup>a</sup> Energy values are reported relative to complex **6** in kcal mol<sup>-1</sup>. <sup>b</sup> Relative energies in methanol, calculated from gas-phase optimized structures using the conductor-like screening model. <sup>c</sup> Gas-phase Gibbs free energies were evaluated at 1 atm of pressure and at 298.15 K.

**Figure 3.** Calculated structure for transition-state **TS4**. Except for the methanol proton, hydrogen atoms are omitted for clarity. Selected bond distances are given in Ångstrom.

pathway B, a palladium assisted intermolecular nucleophilic attack of methanol on acyl species **2**, we obtained a transition-state structure **TS4** (Figure 3). In the transition state, the Pd–ethanoyl bond and the O–H bond of the incoming methanol are elongated and a new Pd–H and C–O bonds are formed simultaneously. The transition state is characterized by the existence of a single imaginary vibrational frequency, corresponding to the proton transfer from the methanol to the palladium center and formation of the carbon–oxygen bond. We subjected the structure to Bader analysis.<sup>37</sup> Bader analysis relies on the topological analysis of the electronic charge density function, and it relates the existence of critical points between atoms to the presence of chemical bonds. In this case, the analysis revealed that the new palladium–hydride and carbon–

oxygen bonds already exist in the transition state, while the palladium–ethanoyl and oxygen–proton bonds are still present. As a consequence, a ring critical point was found, a topology that is in line with the concerted nature of this transition state.

For this metathesis type process we calculate a considerable barrier of 35.8 kcal mol<sup>-1</sup> and a free energy of activation of 43.3 kcal mol<sup>-1</sup>. Taking into account the relatively low stability of  $\eta^2$ -acyl complex **2**, the overall activation energy for methanolysis of complex **6** via this mechanism amounts to 55.8 kcal mol<sup>-1</sup>, and the free energy of activation of the process is 49.8 kcal mol<sup>-1</sup>. These results are in line with previous theoretical studies that show that processes involving proton transfer to Pd(II) centers are highly unfavorable. As a result, these studies have proposed alternative mechanisms involving proton transfer to one of the ligands coordinated to the metal center.<sup>38</sup>

For reductive elimination pathway C, both associative and dissociative pathways for the formation of methanol complex **8** from carbonyl complex **6** were considered. In contrast to carbon monoxide–ethene exchange, no stable trigonal bipyramidal structures were obtained for carbon monoxide–methanol exchange. A linear transit calculation simulating the axial attack of methanol on complex **6** revealed a repulsive interaction. Furthermore, no elongation of the palladium–carbon monoxide bond is observed during this calculation, not even at a palladium–methanol distance of 1.85 Å. Since the axial d-orbital is filled in square planar palladium(II) complexes, the initial orbital interaction between this orbital and the filled  $\sigma$ -orbital of the incoming axial ligand is unfavorable.<sup>39</sup> The initial favorable interaction between complex **6** and the incoming ethene ligand, needed for the formation of five-coordinated intermediate **7**, is not the  $\sigma$ -donation from the ligand to the metal, but rather the back-donation from the filled palladium  $d_{\pi}$ -orbitals to the  $\pi^*$ -orbitals of the ligand. The absence of low-energy  $\pi^*$ -orbitals in the methanol ligand prevents axial coordination of

(37) (a) Bader, R. W. F. *Atoms in Molecules: A Quantum Theory*; Clarendon Press: Oxford, 1994. (b) Ortiz Alba, J. C.; Bo, C. *Xaim-1.0*; Universitat Rovira I Virgili: Tarragona, Spain; <http://www.quimica.urv.es/XAIM>.

(38) (a) Milet, A.; Dedieu, A.; Kapteijn, G.; Van Koten, G. *Inorg. Chem.* **1997**, *36*, 3223. (b) Kragten, D. D.; Van Santen, R. A.; Lerou, J. J. *J. Phys. Chem.* **1999**, *103*, 80. (c) Ng, S. M.; Zhao, C.; Lin, Z. *J. Organomet. Chem.* **2002**, *662*, 120. (d) Mota, A. J.; Dedieu, A.; Bour, C.; Suffert, J. *J. Am. Chem. Soc.* **2005**, *127*, 7171. (e) Davies, D. L.; Donald, S. M. A.; Macgregor, S. A. *J. Am. Chem. Soc.* **2005**, *127*, 13754. (f) Garcia-Cuadrado, D.; Braga, A. A. C.; Maseras, F.; Echavarren, A. M. *J. Am. Chem. Soc.* **2006**, *128*, 1066. (g) Keith, J. A.; Osgaard, J.; Goddard, W. A., III. *J. Am. Chem. Soc.* **2006**, *128*, 3132.

(39) Richens, D. T. *Chem. Rev.* **2005**, *105*, 1961.

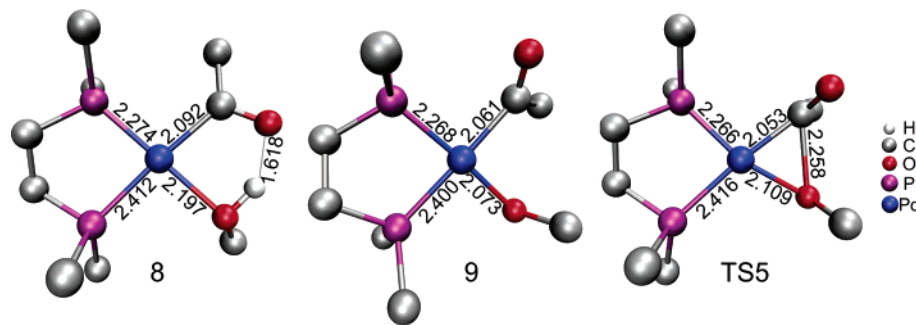


**Figure 4.** Calculated structures for methanolysis of complex **6** via the pathway C. Except for the methanol proton, hydrogen atoms are omitted for clarity. Selected bond distances are given in Ångstrom.

methanol to complex **6**. Furthermore, the electrostatic attraction between the incoming methanol molecule and the cationic palladium complex is small because of the high electron density at the metal center induced by the  $\sigma$ -donating diposphine and ethanoyl ligands. Therefore, it seems that, in contrast to carbon monoxide–ethene exchange, carbon monoxide–methanol exchange cannot proceed through five-coordinated intermediates or transition states. Consequently, formation of methanol complex **8** proceeds through a dissociative process, via complex **2**.

The calculated structure of methanol complex **8** is shown in Figure 4. It exhibits an intramolecular hydrogen bond between the coordinated methanol species and the ethanoyl moiety. Complex **8** is predicted to be significantly less stable than carbonyl complex **6**, but the calculated free energy is comparable to the value predicted for ethene complex **3**.

Deprotonation of the coordinated methanol species in complex **8** leads to the formation of methoxy complex **9**. In protic solvents such as methanol, the deprotonating agent is probably the solvent, while in aprotic solvents, anions present in the reaction mixture might be involved. To evaluate the energetics of the subsequent deprotonation step, it was assumed that the proton of the coordinated methanol moiety is transferred to a cluster of five methanol molecules. The use of a methanol cluster of limited size to describe the acid–base properties of the experimental reaction mixture obviously represents a considerable approximation. Hwang and Chung have recently calculated the solvation free energy of a proton in methanol using small methanol clusters combined with an implicit solvation model, and they observed that the calculated free energy value converged when clusters of at least four explicit methanol molecules were employed in the calculations.<sup>40</sup> The small cluster of explicit methanol molecules accounts for the effects of hydrogen bonding on the stability of the solvated proton and the implicit solvation model stabilizes the positive charge of the overall system. Both in the gas phase and in solution, deprotonation of methanol complex **8** by the solvent is thermodynamically unfavorable. A relative energy of 41.0 kcal mol<sup>-1</sup> is predicted for methoxy complex **9** in the gas phase, while in solution a relative energy of 38.9 kcal mol<sup>-1</sup> is predicted.

As we have previously shown for a similar catalyst system,<sup>7</sup> methoxy complex **9** readily undergoes reductive elimination, via transition-state **TS5**. Also for this more realistic catalyst system, little deformation is observed in the transition state, and

the calculated barrier for ester formation from complex **9** is extremely low (2.3 kcal mol<sup>-1</sup>). The calculated overall free energy barrier for the stepwise methanolysis of carbonyl complex **6** is 41.9 kcal mol<sup>-1</sup>. This value is lower than the calculated barrier for methanolysis pathway B but still considerably higher than the barrier for ethene insertion.

The relatively high energy of methoxy complex **9** and the low barrier for the subsequent ester formation prompted us to investigate a mechanism in which proton transfer and reductive elimination occur in a concerted fashion (pathway D in Scheme 4). In this mechanism, a chain of solvent molecules acts as a proton transfer agent. Studies by Siegbahn have previously shown that solvent mediated proton-transfer mechanisms play an important role in the formation of carbon–oxygen bonds via the palladium catalyzed Wacker reaction.<sup>41</sup> They observed a significant decrease in the activation energy for the nucleophilic attack of water on a palladium coordinated ethene moiety upon introduction of a “proton shuttle” consisting of several solvent molecules.

We propose that methanolysis via pathway D involves the formation of a methanol complex **10**, in which additional methanol molecules are hydrogen-bonded to the coordinated methanol species and the oxygen atom of the ethanoyl moiety (Figure 5). A minimum of two additional methanol molecules was required to transfer the proton from the coordinated methanol species to the apical position of the metal center. As a consequence, the relative energy and Gibbs free energy of complex **10** (Table 2) were evaluated relative to  $\eta^2$ -acyl complex **2** and a small cluster of three methanol molecules (Figure 5). This small cluster is needed to conserve the number of atoms in the reaction, and it was chosen in such a way that it maximizes the number of hydrogen bonds. Note that evaluating the solvation energy of a proton in liquid methanol was a more complex issue and required considering a larger cluster. For the subsequent reductive elimination reaction we obtained transition-state structure **TS6**. The structure is consistent with a late transition state in which both the palladium–ethanoyl and palladium–methanol bonds are elongated and the carbon–oxygen distance is relatively short. The two additional solvent molecules are bridged between the eliminating ester product and one of the axial positions of the palladium complex. Frequency analysis revealed a single imaginary frequency corresponding to reductive elimination of the ester product and transfer of the excess proton via the “proton shuttle” to the palladium center. Clearly, the interplay between the palladium

(40) Hwang, S.; Chung, D. S. *Bull. Korean Chem. Soc.* **2005**, *26*, 589.

(41) (a) Siegbahn, P. E. M.; Stromberg, S.; Zetterberg, K. *Organometallics* **1996**, *15*, 5542. (b) Siegbahn, P. E. M. *J. Phys. Chem.* **1996**, *100*, 14672.

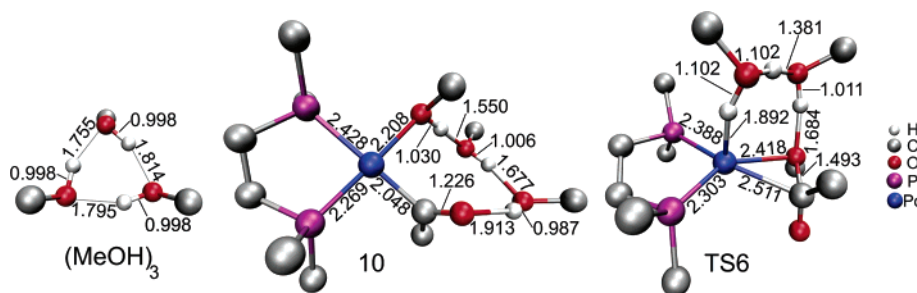


**Figure 5.** Calculated structures for methanolysis of complex **6** via a concerted proton transfer and reductive-elimination pathway. Except for the methanol protons, hydrogen atoms are omitted for clarity. Selected bond distances are given in Ångström.

complex and the solvent is crucial in this mechanism. Proton transfer from the coordinated methanol moiety to the solvent allows reductive elimination of the ester product. During the elimination process, electron density is transferred from the two eliminating moieties to the metal center, increasing the basicity of the complex. This in turn facilitates the transfer of the excess proton from the solvent to the metal.

The barrier for this concerted process is still high ( $34.2 \text{ kcal mol}^{-1}$ ), but it is  $9.1 \text{ kcal mol}^{-1}$  lower than the activation energy of the stepwise proton transfer/reductive elimination pathway C. Note that incorporation of implicit solvation effects using COSMO stabilizes cationic intermediates **6** and **2** relative to **TS6**, which results in only minor differences between the overall activation energies of the stepwise and concerted methanolysis mechanisms in solution. It should be noted that experimentally the reaction mixture is highly complex, containing not only methanol, but also the reactants and products as well as a large excess of a strong acid. Clearly, the addition of acid to the reaction mixture may have a profound influence on the relative rates of the different methanolysis pathways. Pathway C will be disfavored by the addition of acid to the reaction medium, while pathway B will be relatively insensitive to the pH of the reaction mixture. Finally, the proton shuttle mechanism D could even benefit from the increased ionic strength of the medium.

The calculated (gas phase) free energy of activation for the lowest-energy methanolysis pathway is  $7.1 \text{ kcal mol}^{-1}$  higher in energy than the calculated barrier for chain propagation via transition-state **TS3**. Therefore, our calculations predict that catalyst systems containing the bis(dimethylphosphino)ethane ligand exhibit a preference for the copolymerization of ethene and carbon monoxide over the methoxycarbonylation of ethene. This preference has indeed been observed experimentally for similar diphosphine ligand systems.<sup>42</sup>

### 2.3. Ligand Effects. 2.3.1. Electronic Bite-Angle Effects.

We have studied the effect of the bite angle of the bidentate phosphine ligand on the relative energies of the intermediates and transition states involved in chain propagation and methanolysis. To this end, four electronically equivalent ligand systems  $(\text{Me})_2\text{P}(\text{CH}_2)_n\text{P}(\text{Me})_2$ , where  $n = 1-4$ , were investigated. The methyl-substituted diphosphine ligands used in this study minimize steric effects, while ensuring a proper description of the electronic properties of real diphosphine ligands.<sup>7</sup> The relative energies and relative gas-phase Gibbs free energies for the chain propagation and chain termination pathways for all four ligands are shown in Tables 3 and 4. The calculated bite angles of the diphosphine ligands in the calculated structures

**Table 3.** Relative Energies for Intermediates in Ethene Insertion and Methanolysis Pathways Containing  $(\text{Me})_2\text{P}(\text{CH}_2)_n\text{P}(\text{Me})_2$  ( $n = 1-4$ ) Ligands<sup>a</sup>

backbone	2	3a	4	8	9	10	TS3	TS4	TS5	TS6
–CH <sub>2</sub> –	21.1	7.1	–8.8	7.5	40.1	–1.9	21.1	55.7	41.8	30.7
–C <sub>2</sub> H <sub>4</sub> –	20.0	8.0	–10.9	9.3	41.0	–0.6	21.0	55.8	43.3	34.2
–C <sub>3</sub> H <sub>6</sub> –	19.1	10.3	–10.6	10.9	39.1	–0.6	21.3	50.9	42.7	30.0
–C <sub>4</sub> H <sub>8</sub> –	18.4	12.4	–11.4	11.9	38.9	–0.7	23.3	46.2	41.6	27.3

<sup>a</sup> Energy values are reported relative to complex **6** in  $\text{kcal mol}^{-1}$ .

**Table 4.** Relative Gibbs Free Energies for Intermediates in Ethene Insertion and Methanolysis Pathways Containing  $(\text{Me})_2\text{P}(\text{CH}_2)_n\text{P}(\text{Me})_2$  ( $n = 1-4$ ) Ligands<sup>a</sup>

backbone	2	3	4	8	9	10	TS3	TS4	TS5	TS6
–CH <sub>2</sub> –	9.1	10.6	–5.6	10.6	40.0	2.0	25.5	51.6	41.9	29.8
–C <sub>2</sub> H <sub>4</sub> –	6.5	11.0	–9.2	10.7	39.0	2.1	24.1	49.8	41.9	31.3
–C <sub>3</sub> H <sub>6</sub> –	5.5	14.3	–9.0	13.4	38.4	2.5	25.1	45.1	42.2	26.4
–C <sub>4</sub> H <sub>8</sub> –	4.5	16.1	–10.3	14.5	36.9	0.8	25.9	41.8	41.0	25.0

<sup>a</sup> Gibbs free energies were evaluated at 1 atm of pressure and at 298.15 K. Values are reported relative to complex **6** in  $\text{kcal mol}^{-1}$ .

are listed in Table 5. Several bite angle effects are observed. Especially for the large bite-angle *dmpp* ( $n = 3$ ) and *dmpb* ( $n = 4$ ) ligands, the high flexibility of these ligands leads to large differences in bite angle between different species. Clearly, the increased flexibility of the ligand backbone allows the stabilization of a wider variety of complex geometries compared to the more rigid *dmpm* ( $n = 1$ ) and *dmpe* ( $n = 2$ ) ligands and will thus affect the overall energy profiles of both the chain propagation and methanolysis mechanisms. Most notably, the relative energy and Gibbs free energy of  $\eta^2$ -acyl complex **2** decreases with increasing bite angle of the diphosphine ligand. For all four ligands studied here, the bite angle increases upon carbon monoxide dissociation from complex **6**, indicating that a large bite angle stabilizes  $\eta^2$ -acyl complex **2**. Consequently, dissociative ligand exchange processes will be more facile for wide-bite-angle diphosphine ligands. The increased stability of complex **2** for wide-bite-angle ligands seems to be in line with previous experimental observations. Shen et al. reported that for the small-bite-angle *dmpe* ligand ( $n = 2$ ), complex **6** can be formed by insertion of carbon monoxide into the palladium–methyl bond, even at low temperatures.<sup>21</sup> In contrast, Whyman and co-workers have reported that for the wide-bite-angle 1,2-bis(di-*t*-butylphosphinomethyl)benzene ligand, complex **6** is not formed under similar reaction conditions.<sup>16</sup> Instead they observed the formation of an alternative acyl complex, where the fourth coordination site is occupied by a solvent molecule. It should be noted that the large steric bulk of this ligand compared to the *dmpe* ligand system also enhances the stability of complex **2**, as we will show in a subsequent section.

(42) Lindner, E.; Schmid, M.; Wald, J.; Queisser, J. A.; Geprags, M.; Wegner, P.; Nachtigal, C. *J. Organomet. Chem.* **2000**, *602*, 173.



**Table 5.** P–Pd–P Bite Angles (deg) of the (Me)<sub>2</sub>P(CH<sub>2</sub>)<sub>n</sub>P(Me)<sub>2</sub> (*n* = 1–4) Ligands in the Structures Involved in Ethene Insertion and the Methanolysis Pathways

backbone	2	3a	4	6	8	9	10	TS3	TS4	TS5	TS6
–CH <sub>2</sub> –	74.2	72.2	73.7	71.8	73.4	69.7	73.6	74.3	77.6	71.9	73.3
–C <sub>2</sub> H <sub>4</sub> –	87.1	84.8	86.3	85.1	85.8	86.0	86.2	86.9	94.5	86.2	93.2
–C <sub>3</sub> H <sub>6</sub> –	97.8	91.8	94.6	93.2	95.8	96.2	96.7	97.0	115.4	96.5	104.6
–C <sub>4</sub> H <sub>8</sub> –	104.8	93.1	97.8	95.9	94.9	98.4	100.6	98.8	130.2	102.8	132.4

Unlike the relative energies of complexes **2**, both the relative energy and Gibbs free energy of ethene complexes **3** increase with increasing natural bite angle of the diphosphine ligand. With the exception of the dmpm ligand (*n* = 1), the bite angles of the diphosphine ligands in complex **3** vary only slightly between the different ligands. Because of the preferential in-plane coordination mode of the ethene ligand in this complex, steric interactions between the diphosphine ligand and the bulky ethene moiety play a role, even for the relatively small methyl-substituted diphosphine ligands used in this study.

Ethene insertion from complex **3** via transition-state **TS3** becomes more facile with increasing bite angle of the ligand. The barrier for ethene insertion starting from ethene complex **3** decreases from 14.0 kcal mol<sup>−1</sup> for the small dmpm ligand (*n* = 1) to 10.9 kcal mol<sup>−1</sup> for the wide-bite-angle dmpb ligand (*n* = 4). This effect is counterbalanced by the destabilization of ethene complex **3** relative to carbon monoxide complex **6**. The overall effect is a destabilization of transition-state **TS3** relative to carbonyl complex **6**. Therefore, the rate of chain propagation decreases with increasing bite angle of the diphosphine ligand.

The barrier for direct methanolysis of η<sup>2</sup>-acyl complex **2** via transition-state **TS4** is very high for all ligands studied here. A pronounced bite-angle trend is observed in the relative energy of **TS4** that correlates well with the ability of the diphosphine ligand to adopt a larger bite angle during the reaction. For the dmpb ligand (*n* = 4), the bite angle increases from 95.9° in complex **6** to 130.2° in transition-state **TS4**. During the reaction, electron density is transferred from the palladium–ethanoyl bond to the new palladium–hydride bond via the metal center. This increases the electrophilicity of the ethanoyl moiety and allows the formation of the new palladium–hydride bond. It was previously shown theoretically for platinum complexes<sup>43</sup> and experimentally for palladium–diphosphine complexes<sup>44</sup> that an increase in the electron density on the metal center is facilitated by increased ligand bite angles. It is reasonable to assume that also here the wide bite angle of the dmpb ligand (*n* = 4) in the transition state stabilizes the higher electron density at the metal center during this process and thus facilitates the reaction.

Similar to the coordination of ethene, methanol coordination, forming complexes **8** and **10**, is thermodynamically less favorable for wide-bite-angle ligands. The destabilization is less pronounced for the methanol complexes than for the ethene complexes **3**. Consequently, the preference of the catalyst for ethene coordination over methanol coordination decreases with an increasing bite angle of the bidentate ligand. Subsequent deprotonation of methanol complex **8**, forming methoxy species **9**, also becomes thermodynamically more favorable when the bite angle of the diphosphine ligand is increased. Furthermore,

from the relative energies of complexes **8** and **9** (Table 3) it is clear that the acidity of methanol complex **8** increases when wide-bite-angle ligands are employed. Reductive elimination of the ester product via transition-state **TS5** is extremely facile for all four ligands and shows the same bite-angle trend in the relative energy as methoxy complex **9**.

For the concerted proton transfer/reductive elimination methanolysis pathway, a similar bite-angle trend is observed. For all four ligands, the bite angle increases considerably during the reaction. The calculated bite angles for the different ligands in transition-state **TS6** (Table 5) are similar to the bite angles of these ligands in the Pd(0)(diphosphine) complexes we reported recently.<sup>7</sup> Clearly, in the transition-state **TS6** the reductive elimination process has considerably increased the electron density at the metal center. Just as we observed for the methanolysis via transition-state **TS4**, this is a prerequisite for proton transfer to the metal center. It illustrates the crucial role of the solvent molecules in this mechanism. They allow reductive elimination of the ester product and proton transfer of the metal center to proceed simultaneously.

For all three methanolysis transition-states **TS4**, **TS5**, and **TS6**, the relative energies decrease with an increasing bite angle of the diphosphine ligand. The transition state for chain propagation shows an opposite trend; the relative energy of **TS3** increases with increasing bite angle. Therefore, the rate of methanolysis increases with increasing bite angle of the diphosphine ligand, while the rate of chain propagation via ethene insertion decreases correspondingly. For the first three ligands (*n* = 1–3), the barrier for ethene insertion is lower than the barrier for methanolysis, leading to the fast and irreversible formation of β-chelate complex **4**. In contrast, for the wide-bite-angle dmpb ligand (*n* = 4), the calculated free energy barrier for methanolysis via transition-state **TS6** is lower than the barrier for ethene insertion via transition-state **TS3**. As a result, formation of β-chelate complex **4** is slow, allowing methanolysis of ethanoyl–carbonyl complex **6** to take place.

**2.3.2. Steric Bite-Angle Effects.** Steric ligand effects in the methoxycarbonylation of ethene are well documented. Several groups have developed highly active catalyst systems based on bulky diphosphine ligands.<sup>12,13</sup> The effect of steric bulk of diphosphine ligands on the chemoselectivity of the catalyst has recently been demonstrated by Pugh and Drent, who compared several alkyl substituted diphosphine ligands based on the 1,2-ethanediyl and 1,3-propanediyl backbones as ligands in the methoxycarbonylation of ethene.<sup>45</sup> The sterically hindered 1,3-bis(di-*t*-butylphosphino)propane ligand yielded methyl propionate exclusively. The less bulky 1,3-bis(di-*s*-butylphosphino)propane and 1,2-bis(di-*t*-butylphosphino)ethane ligands, on the other hand, preferred ethene insertion over methanolysis. In the presence of hydrogen, these ligands yielded highly active and selective catalysts for the formation of 3-pentanone.

(43) Otsuka, S. *J. Organomet. Chem.* **1980**, *200*, 191.(44) (a) Berning, B. E.; Noll, B. C.; DuBois, D. *J. Am. Chem. Soc.* **1999**, *121*, 11432. (b) Raebiger, J. W.; Miedaner, A.; Curtis, C. J.; Miller, S. M.; Anderson, O. P.; DuBois, D. *J. Am. Chem. Soc.* **2004**, *126*, 5502.(45) Pugh, R. I.; Drent, E. *Adv. Synth. Catal.* **2002**, *344*, 837.

**Table 6.** Relative Energies for Intermediates in Ethene Insertion and Methanolysis Pathways Containing  $(t\text{-Bu})_2\text{P}(\text{CH}_2)_n\text{P}(t\text{-Bu})_2$  Ligands ( $n = 1\text{--}4$ )<sup>a</sup>

backbone	2	3	8	9	10	TS3	TS4	TS5	TS6
–CH <sub>2</sub> –	19.1	10.3	8.9	38.6	–1.0	22.6	52.9	38.0	33.6
–C <sub>2</sub> H <sub>4</sub> –	16.2	14.9	11.8	39.2	–1.3	25.4	50.2	41.5	33.2
–C <sub>3</sub> H <sub>6</sub> –	11.7	21.0	10.9	42.2	3.7	30.1	41.1	39.5	34.5
–C <sub>4</sub> H <sub>8</sub> –	14.7	22.2	23.7	43.8	8.0		33.2		48.5

<sup>a</sup> Energy values are reported relative to complex **6** in kcal mol<sup>–1</sup>.

We have investigated diphosphine ligands  $(t\text{-Bu})_2\text{P}(\text{CH}_2)_n\text{P}(t\text{-Bu})_2$ , where  $n = 1\text{--}4$ , using hybrid quantum mechanics/molecular mechanics calculations. To facilitate comparison between the methyl and *t*-butyl substituted ligand systems, the QM-part of the QM/MM calculations consisted of the  $(\text{Me})_2\text{P}(\text{CH}_2)_n\text{P}(\text{Me})_2$  ligand as well as the palladium center and other ligands connected to the metal center. The methyl groups of the *t*-butyl moieties were treated at the molecular-mechanics level. Since the QM/MM methodology we employed does not allow electronic coupling between the QM and MM part of the system, changes in the electronic properties of the diphosphine ligand are kept to a minimum, and this allows us to isolate effects caused by the steric bulk of the ligand. The relative energies for the chain propagation and methanolysis pathways for all four ligands are shown in Table 6. For the large bite angle  $(t\text{-Bu})_2\text{PC}_4\text{H}_8\text{P}(t\text{-Bu})_2$  ligand highly distorted structures are obtained. Furthermore, we are unable to locate transition-state structures **TS5-*t*Bu** and **TS3-*t*Bu** for this ligand. Invariably, reductive elimination and ethene insertion products were obtained, respectively. Structures **6-*t*Bu**, **3-*t*Bu** and **9-*t*Bu** exhibit unusually long palladium–phosphorus bond distances of 2.7–3.0 Å trans to the ethanoyl moiety, while for complexes **8-*t*Bu**, **2-*t*Bu** and **TS4-*t*Bu**, the bidentate coordination of the diphosphine ligand remains unaffected. This supports previous experimental observations that these bulky ligand systems have a high tendency to open the chelate ring and form polymeric palladium species containing bridging diphosphine ligands.<sup>13,19</sup> No significant elongation of the palladium–phosphorus bond trans to the ethanoyl moiety is found for complexes containing the other three *t*-butyl substituted ligands ( $n = 1\text{--}3$ ). Since for ligand  $n = 3$  also exclusively methyl propionate is obtained experimentally, Pd–P bond lengthening does not seem to be a prerequisite for the fast formation of methyl propionate.

Several effects induced by the addition of sterically demanding substituents to the phosphine moieties are observed. The *t*-butyl groups clearly stabilize three-coordinated complex **2-*t*Bu** relative to carbonyl complex **6-*t*Bu** and enhance the bite-angle trend observed for the complexes containing methyl-substituted ligands. Taking into account the stabilization of complex **2** ascribed to entropic effects calculated for the methyl substituted ligands (12–14 kcal mol<sup>–1</sup>), it is highly likely that for the two large-bite-angle ligands ( $n = 3, 4$ ) carbonyl complex **6-*t*Bu** is less stable than complex **2-*t*Bu**, in line with experimental observations.<sup>16</sup>

The destabilization of ethene complexes **3**, relative to complex **6**, is even more pronounced for the *t*-butyl-substituted ligands than for the methyl-substituted ligands. The increased steric hindrance induced by the *t*-butyl-substituted ligands overcomes the electronic preference for an in-plane coordination mode of the ethene ligand observed for the much smaller methyl-

substituted ligand systems. Except for the small-bite-angle bis-(*di-t*-butylphosphino)methane ligand, the lowest energy structures for **3-*t*Bu** exhibit coordination of the ethene moiety perpendicular to the plane of the complex. Since insertion of ethene into the palladium–ethanoyl bond requires a nearly in-plane orientation of ethene moiety, it is not surprising that the relative energy of transition-state **TS3-*t*Bu** increases as the bite angle and steric hindrance induced by the diphosphine ligand increase. Consequently, the use of bulky diphosphine ligands inhibits the formation of  $\beta$ -chelate complex **4** via ethene insertion, as was observed by Drent and co-workers.

The increase in the relative energy of methanol complex **8-*t*Bu** is similar to the destabilization observed in the complexes containing methyl substituted ligands **8**. For the  $(t\text{-Bu})_2\text{PC}_3\text{H}_6\text{P}(t\text{-Bu})_2$  ligand ( $n = 3$ ), a different structure that exhibits no intramolecular hydrogen-bonding interaction between the ethanoyl moiety and the coordinated methanol ligand is predicted. This geometry minimizes steric repulsion between the diphosphine ligand and the methanol and ethanoyl moieties of complex **8-*t*Bu**. The structure is 1.2 kcal mol<sup>–1</sup> more stable than the structure containing the intramolecular hydrogen bond. This absence of an intramolecular hydrogen bond enhances the interaction between the proton of the coordinated methanol ligand and the deprotonating agent (i.e., the solvent or anions), possibly enhancing proton transfer. The energies of neutral methoxy complex **9-*t*Bu** relative to the carbonyl complex **6** change little between the methyl- and *t*-butyl-substituted ligands. Clearly, the carbon monoxide ligand in complex **6** and the methoxy species in complex **9** impose a similar amount of steric hindrance. Also the barrier for the subsequent reductive elimination of the final product via transition-state **TS5** remains essentially unchanged. Therefore it seems that the addition of bulky substituents to the diphosphine ligand has little effect on the overall barrier for ester formation via a stepwise proton transfer/reductive elimination pathway.

Methanolysis via nucleophilic attack of methanol to complex **2-*t*Bu**, through transition-state **TS4-*t*Bu**, is strongly favored by the increased stability of both complex **2-*t*Bu** and transition-state **TS4-*t*Bu** for systems containing bulky *t*-butyl-substituted ligands. The bite-angle trend observed for the stability of transition-state **TS4** containing methyl-substituted ligands is further enhanced by the addition of steric bulk. Since the carbon–oxygen bond-forming process in transition-state **TS4** occurs relatively far from the metal center (Figure 3), steric repulsion between the two reacting moieties and the bulky diphosphine ligand is small. Furthermore, the increased bite angle of the diphosphine ligand in transition-state **TS4** compared to square planar carbonyl complex **6** minimizes steric interactions among the different *t*-butyl groups of the diphosphine ligand. As a result, nucleophilic attack via transition-state **TS4-*t*Bu** effectively competes with the other methanolysis pathways for the bulky wide-bite-angle ligands studied here. Not surprisingly, the highly congested transition-state structure **TS6** for the concerted proton transfer/reductive elimination methanolysis pathway is disfavored by the addition of bulky groups to the diphosphine ligands. The bulky *t*-butyl substituents induce significant steric hindrance around the axial positions of the square planar palladium complexes, thereby disfavoring coordination of the solvent chain to the axial position of the palladium complex in transition-state **TS6-*t*Bu**.

Although sterically bulky ligands clearly enhance methanolysis via transition-state **TS4-*t*Bu**, a similar trend is not observed in the other two methanolysis pathways. The experimentally observed intrinsic rate enhancement for methanolysis involving bulky wide-bite-angle diphosphine ligands compared to less bulky ligands, however, could also originate from a change in resting state of the catalyst. Ethene coordination to palladium–ethanoyl complexes and subsequent (irreversible) insertion into the growing polymer chain are strongly inhibited by the use of bulky diphosphine ligands, “trapping” ethanoyl complexes **6-*t*Bu** and **2-*t*Bu**. In turn, this increase in the concentration of ethanoyl complexes **6-*t*Bu** and/or **2-*t*Bu** in the reaction medium for wide-bite-angle bulky ligands enhances the rate of methanolysis. So while less bulky ligands yield fast formation of  $\beta$ -chelate complex **4** (which is committed to the formation of copolymer), sterically congested diphosphine ligands induce fast formation of ester products via the methanolysis of palladium–ethanoyl complexes.

### 3. Conclusions

We have studied both the chain-propagation mechanism and methanolysis chain-termination mechanisms of the alternating copolymerization of ethene and carbon monoxide, catalyzed by palladium complexes containing electron-donating diphosphine ligands. The rate determining step in the chain-propagation mechanism is the insertion of ethene into the palladium–ethanoyl bond, yielding  $\beta$ -chelate complex **4**. Although ethene insertion starting from ethene complex **3a** is facile, the relatively low affinity of the catalyst for coordination of the electron donating ethene ligand compared to carbon monoxide increases the overall free-energy barrier for chain propagation to 24.1 kcal mol<sup>-1</sup>.

We have shown that for the methanolysis pathways considered in this study, formation of  $\eta^2$ -acyl intermediate **2** is crucial. The palladium-assisted nucleophilic-attack pathway requires a vacant site adjacent to the ethanoyl moiety, and methanol complexes **8** and **10** do not form from carbonyl complex **6** through associative ligand exchange processes. For all methanolysis pathways considered in this study, relatively high barriers are obtained for the formation of the final ester product, in agreement with experimental observations for (Me)<sub>2</sub>P(CH<sub>2</sub>)<sub>*n*</sub>P-(Me)<sub>2</sub> ligand systems. Our calculations show that the most likely methanolysis pathway involves a proton-transfer/reductive-elimination mechanism, in which the solvent acts as a proton-transfer agent. Having established the mechanisms of chain propagation and methanolysis for palladium-based catalysts containing electron-donating diphosphine ligands, we subsequently investigated effects caused by changes in the bite angle and steric bulk of the diphosphine ligand on the rates of chain propagation and methanolysis reactions. Several effects have been observed:

(1) Both increasing the bite angle and increasing the steric bulk of the diphosphine ligand stabilizes  $\eta^2$ -acyl complex **2**, a crucial intermediate in all methanolysis pathways considered in this study.

(2) Increasing the steric bulk of the ligand strongly disfavors the formation of ethene complex **3** and consequently increases the barrier for ethene insertion via transition-state **TS3**.

(3) For all three methanolysis pathways considered in this study, increasing the bite angle of the diphosphine ligand

increases the rate of methanolysis. This is attributed to the involvement of electron-rich intermediates and/or transition states in all three methanolysis pathways.

(4) The steric bulk of the diphosphine ligand hardly affects the barriers for methanolysis via the stepwise and concerted reductive-elimination pathways. Transition-state **TS4** for the direct nucleophilic attack of methanol on complex **2**, discarded for non-bulky ligands, is stabilized by increasing steric bulk of the diphosphine ligand.

(5) For the highly bulky but flexible 1,4-bis(di-*t*-butylphosphino)butane ligand, significant bond-lengthening of one of the arms of the bidentate ligand during the catalytic cycle was calculated.

On the basis of these observations, we postulate that the high activity and chemoselectivity in the methoxycarbonylation of ethene observed for *t*-butyl-substituted wide-bite-angle diphosphine ligands is determined by a combination of electronic and steric effects induced by the diphosphine ligand. The high electron density at the metal center induced by the  $\sigma$ -donating diphosphine ligand stabilizes  $\eta^2$ -acyl intermediate **2**, while suppressing the formation of 18-electron intermediates such as ethene complex **7**. The electronic stabilization of complex **2** is enhanced by increasing the steric bulk and increasing the bite angle of the diphosphine ligand. Simultaneously, the high electron density at the metal center and steric bulk of the diphosphine ligand strongly disfavor ethene coordination to the metal center, preventing fast ethene insertion into the growing polymer chain. In comparison, methanol coordination is hardly affected by the steric bulk of the ligand, and direct nucleophilic attack of methanol on  $\eta^2$ -acyl complex **2** is even enhanced by increasing steric bulk of the ligand. Furthermore, for all three methanolysis pathways considered in this study, the barrier for the formation of the ester product decreases when the bite angle of the diphosphine ligand increases. For all three pathways, this is attributed to the formation of zerovalent palladium complexes, which are stabilized by wide-bite-angle ligands.

Our computational studies support the experimental work that steric bulk of bidentate phosphine ligands strongly favors ester formation over polymerization. In addition our studies confirm our intuitive conclusion that wide bite angles lead to low-molecular-weight products as they give faster reductive elimination in C–X bond formation than small-bite-angle diphosphines. This is closely related to ligand effects in palladium- and nickel-catalyzed cross-coupling reactions, at least for those instances where the reductive elimination is the rate-determining step.<sup>7,31,32,46</sup>

### 4. Experimental Section

All DFT calculations were performed using the Amsterdam density functional program (ADF2004.01) developed by Baerends et al.<sup>47</sup> using the local density approximation of Vosko, Wilk, and Nusair<sup>48</sup> and the nonlocal gradient correction of Becke and Perdew.<sup>49</sup> Relativistic corrections were introduced by scalar-relativistic zero-order regular

(46) Kranenburg, M.; Kamer, P. C. J.; Van Leeuwen, P. W. N. M.; Vogt, D.; Keim, W. *J. Chem. Soc., Chem. Commun.* **1995**, 2177.

(47) (a) Baerends, E. J.; et al. *ADF*, version 2004.01; Scientific Computing and Modeling: Amsterdam, The Netherlands, 2004; <http://www.scm.com>. (b) Guerra, C. F.; Snijders, J. G.; Te Velde, G.; Baerends, E. J. *Theor. Chem. Acc.* **1998**, *99*, 391.

(48) Vosko, S. H.; Wilk, L.; Nusair, M. *Can. J. Phys.* **1980**, *85*, 1200.

(49) (a) Becke, A. D. *Phys. Rev. A: At., Mol., Opt. Phys.* **1988**, *38*, 3098. (b) Perdew, J. P. *Phys. Rev. B: Condens. Matter Mater. Phys.* **1986**, *33*, 8822.

approximation (ZORA).<sup>50</sup> A triple- $\zeta$  plus polarization basis set was used on all atoms. For non-hydrogen atoms a relativistic frozen-core potential was used, including 3d for palladium, 2p for phosphorus and 1s for carbon and oxygen. A general numerical integration parameter of 6.0 was employed in all calculations.

All optimized structures were subjected to frequency analysis. The energy minima structures were characterized by the absence of imaginary frequencies, while the transition-state structures exhibited a single imaginary frequency that corresponded to the reaction coordinate. Gibbs free energies were calculated at a temperature of 298.15 K and a pressure of 1.0 atm. Solvation energies of gas-phase optimized structures were calculated using the conductor-like screening model (COSMO)<sup>51</sup> as implemented in the ADF program.<sup>52</sup> Calculations were performed using a dielectric constant of 33.6 for methanol. Solvent-excluding surfaces were generated using a solvent radius of 2.00 Å. Van der Waals radii of 1.6 Å for palladium, 1.80 Å for phosphorus, 1.70 Å for carbon, 1.52 Å for oxygen, and 1.20 Å for hydrogen atoms were employed.

The QM/MM calculations were performed in ADF, using the IMOMM method developed by Maseras and Morokuma<sup>53</sup> and implemented by Woo et al.<sup>54</sup> The QM-part consisted of the previously optimized complexes while the MM-part was described using the TRIPOS 5.2 force field,<sup>55</sup> which was modified to include the Van der

Waals radius for palladium taken from the UFF force field.<sup>56</sup> Hydrogen was chosen as link-atom and the link-bond parameter was set to 1.39. This value was obtained by dividing the average carbon-carbon bond distance of the *t*-butyl groups of the 1,2-bis(di-*t*-butylphosphinomethyl)-benzene ligand (dtbpm) in the crystal structure of Pd(dtbpmb)(C(O)-Et)Cl<sup>16</sup> by the average carbon-hydrogen bond distance for the methyl groups in the calculated structures containing methyl-substituted diphosphine ligands. A simple electrostatic coupling model was employed, not allowing polarization of the QM-wavefunction by the MM-part of the calculation. Bader analysis of transition-state **TS4** was performed using the XAIM program developed by Bo and co-workers.<sup>37a</sup>

**Acknowledgment.** This work was supported by The Netherlands Organization for Scientific Research (NWO/CW). We are indebted to the MEC of the Government of Spain (Grants CTQ2005-06909-C02-02/BQU and CSD2006-0003), to the CIRIT of the Catalan Government (Grant 2005SGR00715), and to the ICIQ Foundation for financial support. The SARA center for high performance computing is acknowledged for use of their computational facilities.

**Supporting Information Available:** Complete ref 47a, calculated structures and energies of all intermediates, and transition states and the imaginary frequencies of the transition states. This material is available free of charge via the Internet at <http://pubs.acs.org>.

JA0684500

- (50) (a) Van Lenthe, E.; Baerends, E. J.; Snijders, J. G. *J. Chem. Phys.* **1993**, *99*, 4597. (b) Van Lenthe, E.; Baerends, E. J.; Snijders, J. G. *J. Chem. Phys.* **1994**, *101*, 9783. (c) Van Lenthe, E.; Ehlers, A. E.; Baerends, E. J.; Snijders, J. G. *J. Chem. Phys.* **1999**, *110*, 8943.
- (51) (a) Klamt, A.; Schuurmann, G. *J. Chem. Soc., Perkin Trans. 2* **1993**, 799. (b) Klamt, A. *J. Phys. Chem.* **1995**, *99*, 9972. (c) Klamt, A.; Jones, V. *J. Chem. Phys.* **1996**, *105*, 9972.
- (52) (a) Pye, C. C.; Ziegler, T. *Theor. Chem. Acc.* **1999**, *101*, 396. (b) Te Velde, G.; Bickelhaupt, M. F.; Baerends, E. J.; Guerra, C. F.; Van Gisbergen, S. J. A.; Snijders, J. G.; Ziegler, T. *J. Comput. Chem.* **2001**, *22*, 931.
- (53) (a) Maseras, F.; Morokuma, K. *J. Comput. Chem.* **1995**, *16*, 1170. (b) Maseras, F. *J. Chem. Soc., Chem. Commun.* **2000**, 1821.
- (54) Woo, T. K.; Cavallo, L.; Ziegler, T. *Theor. Chem. Acc.* **1998**, *100*, 307.

- (55) (a) Singh, U. C.; Kollman, P. A. *J. Comp. Chem.* **1986**, *7*, 718. (b) Clark, M.; Cramer, R. D., III; Van Opdenbosch, N. *J. Comp. Chem.* **1989**, *10*, 982.
- (56) Rappe, A. K.; Casewit, C. J.; Colwell, K. S.; Goddard, W. A., III. *J. Am. Chem. Soc.* **1992**, *114*, 10024.